

Supporting Information

Safe preparation, energetic performance and reaction mechanism of corrosion-resistant Al/PVDF nanocomposite films

Xiang Ke^a, Shuangfeng Guo^b, Gensheng Zhang^c, Xiang Zhou^{a,*}, Lei Xiao^a, Gazi, Hao^a,
Ning Wang^a, and Wei Jiang^{a,*}

^a National Special Superfine Powder Engineering Research Center, Nanjing University of Science and Technology, Nanjing, China

^b Xi'an Modern Chemistry Research Institute, Xi'an, China

^c Shanxi Jiangyang Chemical Co., Ltd, Taiyuan, China

Content

1. Calculation of the active Al content in Al NPs
2. Experimental apparatus of combustion test
3. Digital photograph of the as-obtained films
4. Cross-sectional SEM images of Al/PVDF films
5. Top-view SEM images of Al/PVDF films
6. AFM images of Al/PVDF films
7. XPS spectra of Al/PVDF films
8. Calculative process of corrosion resistance
9. Corrosion-resistance experiments in water
10. Calculating process of Al NPs after thermal analysis
11. DSC curve of pure PVDF film
12. TGA-DSC test of Al₂O₃/PVDF films
13. Optical signal during the combustion process

1. Calculation of the active Al content in Al NPs

In order to analyze the active Al content, TGA analysis is conducted from 50 to 1000 °C with a heating rate of 10 °C min⁻¹ under an air flow rate of 50 mL min⁻¹ and kept at 1000 °C for 30 minutes to ensure that Al NPs are completely oxidized. The reaction of the Al in air is shown as



The TGA curve is shown in **Fig.S1** and the mass gain in the TGA is attributed to oxidation of active aluminum. The active aluminum content (*c*) can be calculated using the following equation:

$$c(\%) = \frac{108}{96} \Delta m(\%) \quad (2)$$

where $\Delta m(\%)$ is the percent mass gain in the TGA experiment. According to results of TGA test, the active aluminum content is 73.38%.

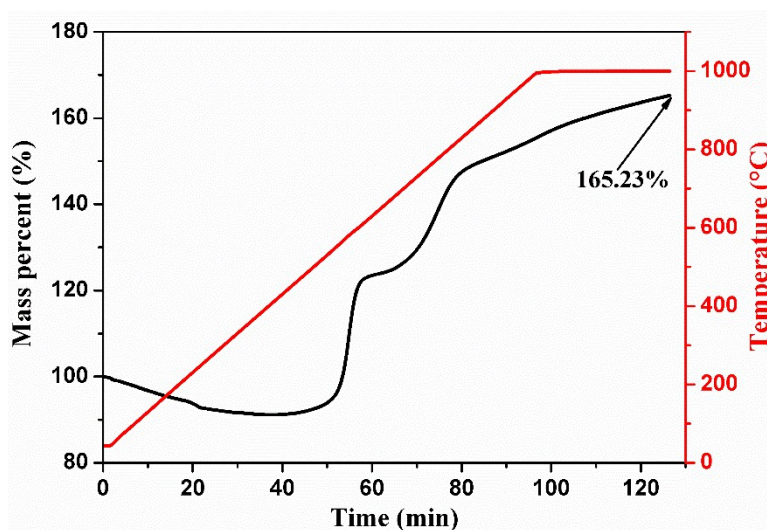


Fig. S1. TGA curve of Al-NPs in air

2. Experimental apparatus of combustion test

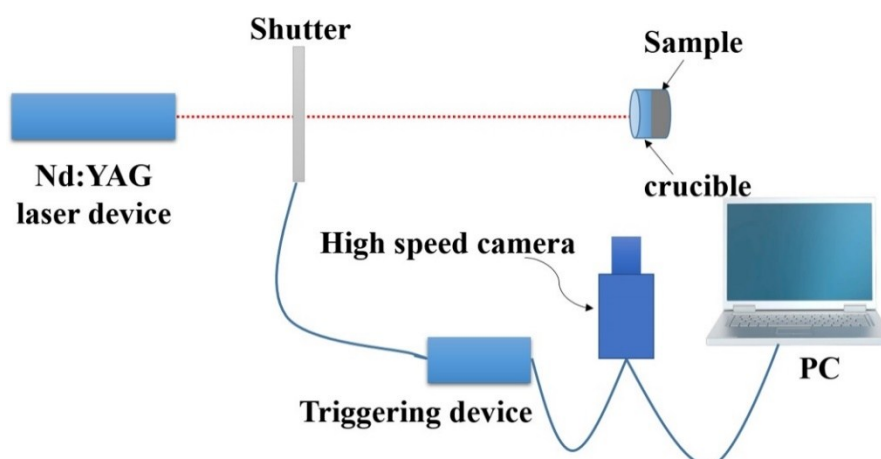


Fig. S2. Schematic diagram of the set of experimental apparatus for recording combustion process.

3. Digital photograph of the as-obtained film

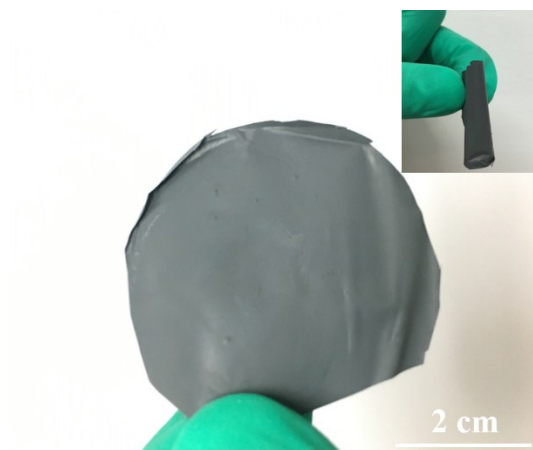


Fig.S3. A digital photograph of Al-30.

4. Cross-sectional SEM images of Al/PVDF films

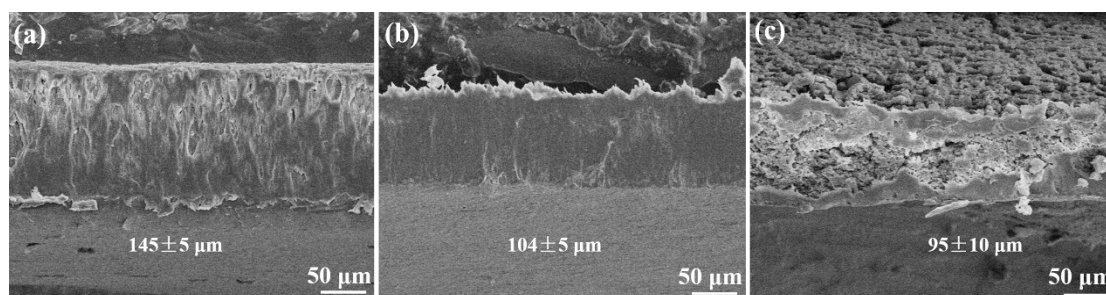


Fig. S4. Cross-sectional SEM images of Al/PVDF films: (a) Al-10, (b) Al-30 and (c) Al-50.

5. Top-view SEM images of Al/PVDF films

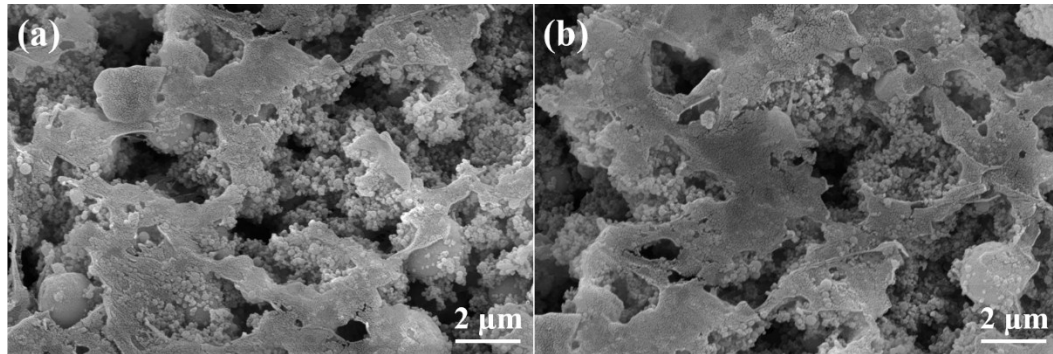


Fig. S5. SEM images of Al/PVDF films: (a) 60% Al and (b) 70% Al

6. AFM images of Al/PVDF films

The 3D and 2D AFM images show the undulant surface of Al/PVDF films, which are well in agreement with the SEM images. The mean surface roughness (Ra) and root mean square roughness (Rq) are increased with the increasing Al loading. The height variation diagram for selected path way (gray line) is shown and the results show that the height rangeability is also increased with the increasing Al loading, in good agreement with the results of surface roughness.

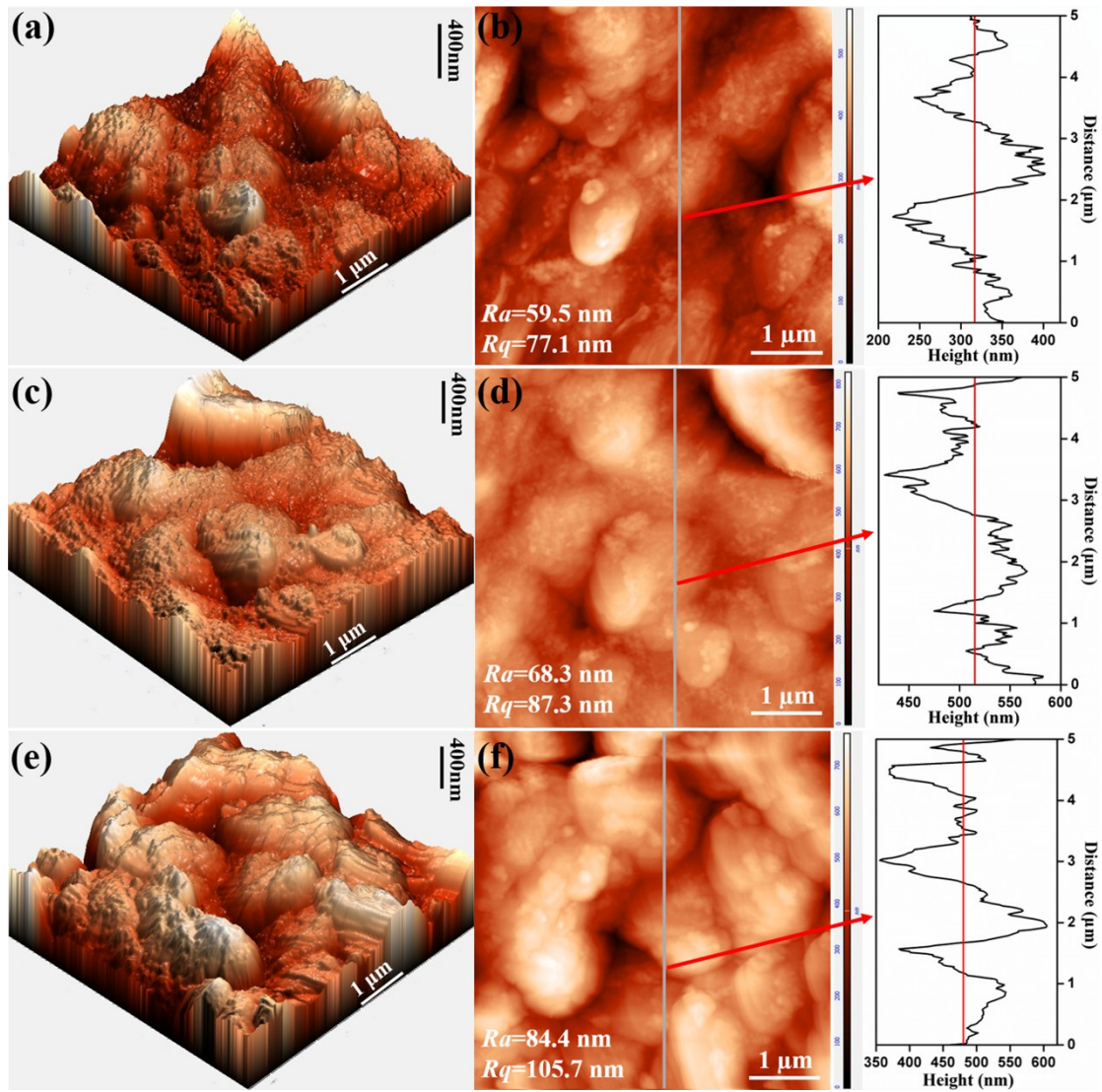


Fig. S6. (a, c and e) 3D and (b, d, and f) 2D AFM images with height variation diagram of Al-10 (a, b), Al-30 (c, d) and Al-50 films (e, f), respectively.

Table S1. Surface roughness and average height of energetic films of Al/PVDF energetic films.

Sample	Surface roughness /nm			
	S_a	S_q	S_z	S_y
Al-10	59.5	77.1	284.8	569.8
Al-30	68.3	87.3	387.2	765.9
Al-50	84.4	105.7	423.3	824.7

S_a : average roughness; S_q : root mean square roughness; S_z : ten-point average roughness, S_y : maximum surface roughness.

7. XPS spectra of Al/PVDF films

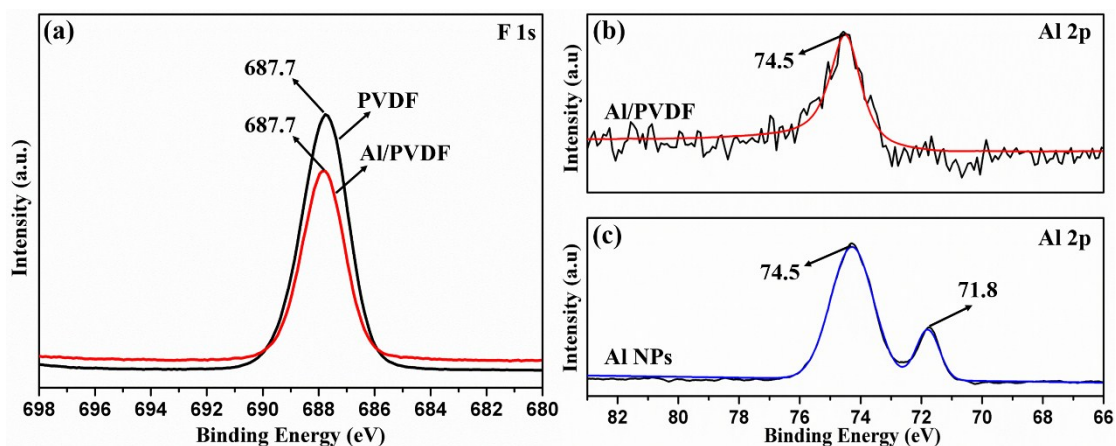
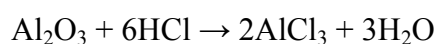
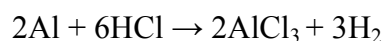
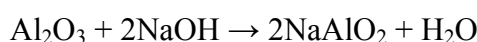


Fig. S7. (a) High-resolution F 1s XPS spectra; (b) and (c) High-resolution Al 2p XPS spectra of Al/PVDF and Al NPs, respectively.

8. Calculative process of corrosion resistance

In consideration of the chemical reaction between Al and NaOH/HCl or between Al₂O₃ shell and NaOH/HCl as below, the products are all easily soluble.



It should be noted that Al₂O₃ shell is ignored in this calculative process because it is hard to confirm its accurate content after reaction. What's more, the Al₂O₃ shell maybe firstly react with the solution because it is outside the Al core. Therefore, the collected film after reaction only includes unreacted Al NPs and PVDF after several cleaning treatments. The weight of pure PVDF film is almost unchanged (99.7%) after soaking in NaOH solution, demonstrating its outstanding chemical stability. Hence, the mass change of PVDF is also ignored and the residual Al NPs is calculated as below.

$$\text{Residual Al} \Big|_{\text{Al-x}} = \frac{M_1 - M_2}{M_3} \times 100$$

Where M_1 , M_2 and M_3 is the weight percent of residual film, initial weight percent of PVDF and initial weight percent of Al NPs, respectively. Then, the calculative process is shown:

$$\text{Residual Al} \Big|_{\text{Al-10}} = \frac{98.78 - 90}{10} \times 100 = 87.8\%$$

$$\text{Residual Al} \Big|_{\text{Al-30}} = \frac{93.32 - 70}{30} \times 100 = 78.43\%$$

$$\text{Residual Al} \Big|_{\text{Al-50}} = \frac{84.27 - 50}{50} \times 100 = 67.54\%$$

The calculative results are shown in Table S1.

Table S2. Results of corrosion-resistance experiments

Sample	Weight percent/%	
	NaOH	HCl
Al	0	3.64± 2.4
Al-10	87.89 ± 1.0	90.12± 1.3
Al-30	78.43± 2.1	81.35± 2.5
Al-50	68.54± 2.2	72.42± 2.7

Although some errors exist in this calculative process, it can still verify the corrosion-resistance capacity of Al/PVDF films in contrast with the weight change of pure Al NPs.

9. Corrosion-resistance experiments in water

As for the corrosion resistance for water, two groups of contrastive experiments have been conducted: one is that the Al NPs or Al/PVDF films are put into deionized water for 5 days at room temperature (25°C), another is that the Al NPs or Al/PVDF films are put into deionized water for 1 h at high temperature (50°C). Noted that the weight change cannot be used as the evaluation criterion because the reaction product (AlO(OH)) of water and Al NPs is insoluble. Therefore, the crystal structure and active Al content are used to estimate the corrosion resistance in water.

Using Al-30 as an example, Fig. S8 shows the digital photographs of Al NPs and Al-30 films before and after corrosion-resistance experiment in water for 1h at 50°C. In Fig. S8, the light black the suspension of Al NPs changes into off-white after corrosion-resistance experiment, while the light black Al-30 films show no change in color, directly revealing their remarkable anti-water performance. The XRD pattern in Fig.

S9a shows that Al NPs have been completely transformed into AlO(OH) after stored in water for 1 h at 50°C, while part of active Al NPs still exist after stored in water for 5 days at 25°C. However, the results of Al-30 films in Fig. S9b demonstrate no change of crystal structure of Al NPs in both corrosion-resistance experiments, suggesting that PVDF can offer protection to Al NPs effectively. Then, from the view of energy, Al NPs lose activity completely after the corrosion-resistance experiment at 50°C. The weight loss in Fig. S9c (red line) is caused by the desorption of water and the transformation from AlO(OH) to Al₂O₃. After stored for 5 days at 25°C, the content of active Al is 37.6%, about half of the fresh Al NPs. Then DSC curves in Fig. S9d also confirm these findings. The TGA curves for both experiments of Al-30 in Fig. S9e show that reactions between the Al and PVDF still happen and the DSC curves in Fig. S9f show the same trend when compared with the fresh Al-30 films, except for slight delay of the exothermic peak temperature. The heat release for the experiments at 50°C and 25°C is 1712 and 1844 J g⁻¹, respectively, about 78.2% and 84.2% of the fresh Al-30 sample. On the basis of above results, Al/PVDF energetic films show their outstanding anti-water, acid-resistant and alkali-resistant properties.

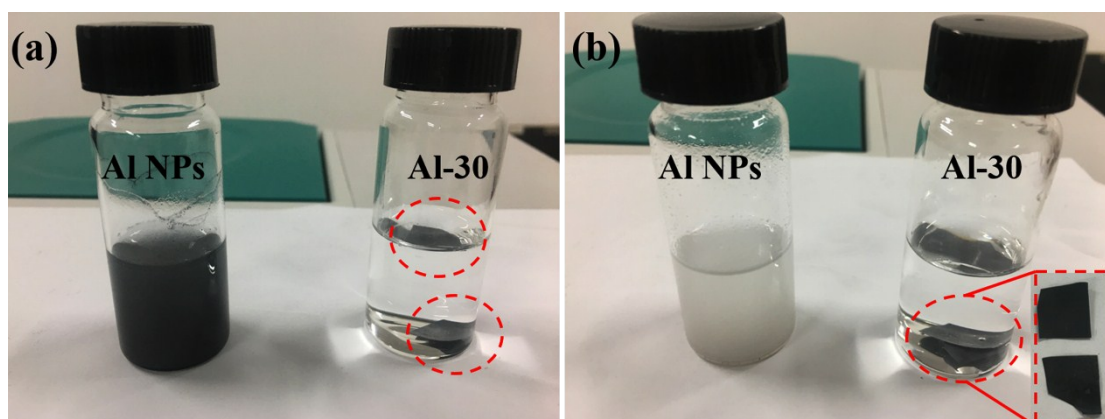


Fig. S8. Digital photographs of Al NPs and Al-30 films (a) before and (b) after corrosion-resistance experiment in water at 50°C.

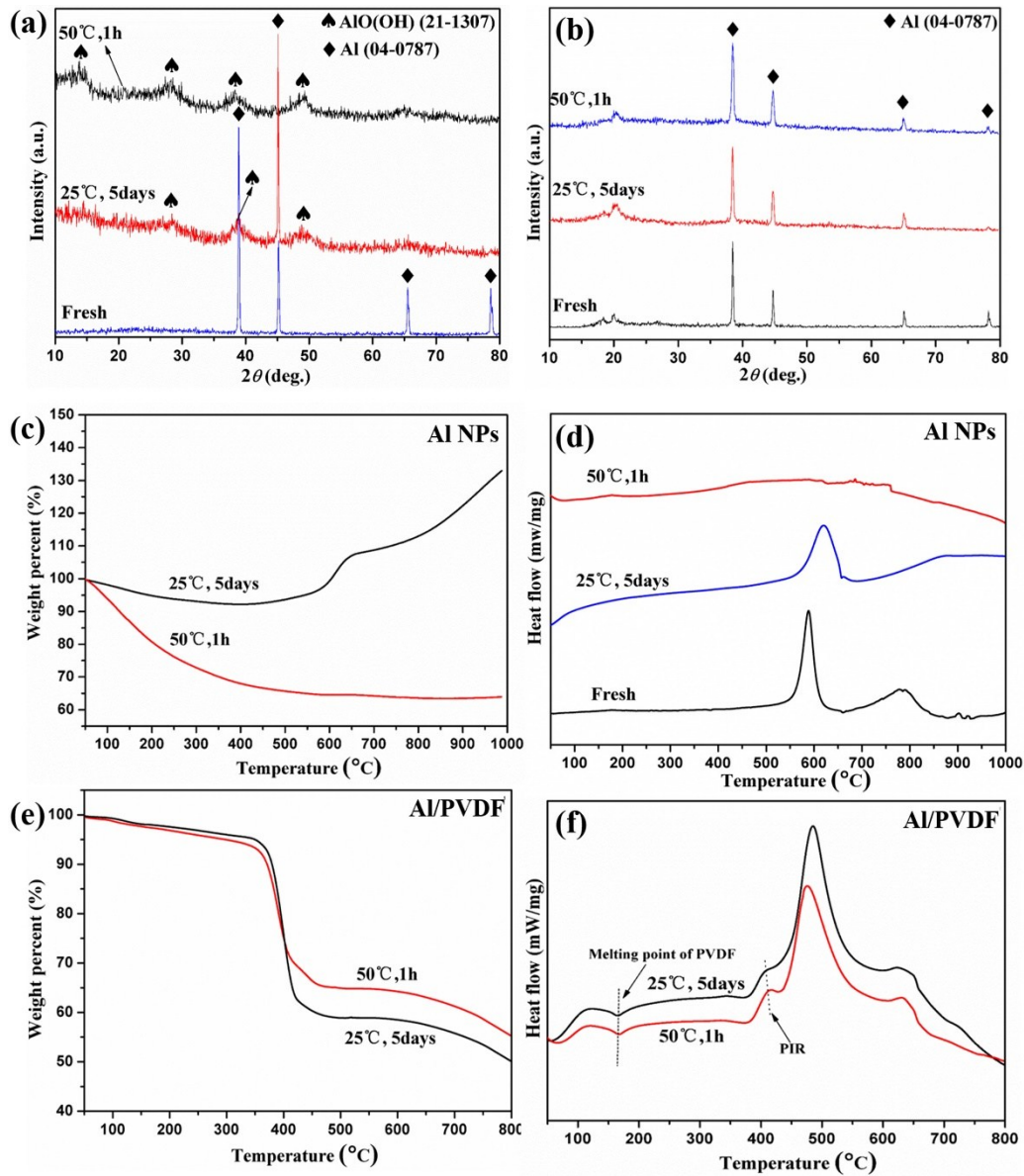


Fig. S9. XRD patterns of (a) Al NPs and (b) Al-30 films after corrosion-resistance experiment; (c) TGA and (d) DSC curves of Al NPs; (e) TGA and (f) DSC DSC curves of Al-30 films after corrosion-resistance experiment.

10. Calculating process of Al NPs after thermal analysis

Based on the residual mass of pure PVDF (30.1% at 500°C), if presuming no reaction between Al NPs and PVDF, the residual mass of PVDF for Al-10, Al-30 and Al-50 would be 27.09, 21.07 and 15.05, respectively. Then, the total residual mass are calculated.

$$\text{Residual mass} \Big|_{Al-10} = 90 \times 0.301 + 10 = 37.1$$

$$\text{Residual mass} \Big|_{Al-30} = 70 \times 0.301 + 30 = 51.1$$

$$\text{Residual mass}_{Al-50} = 50 \times 0.301 + 50 = 65.0$$

Table S3. Residual mass of Al/PVDF energetic films at 500 °C

Sample	Primal mass /%		Residual mass /%	
	PVDF	Al	Theoretical value	Actual value
Al-10	90	10	37.1	56.3
Al-30	70	30	51.1	62.9
Al-50	50	50	65.0	73.1

11. DSC curve of pure PVDF film

The endothermic peak from 140 to 190 °C is due to the melting of PVDF and the exothermic peak starting from 465 °C is attributed to the main decomposition of PVDF, which is in line with the main weight loss in the TGA curve. The peak temperature in DSC curve is about 505 °C, which agrees well with the end temperature in TGA curve, indicating that the heat release is caused by the decomposition of PVDF.

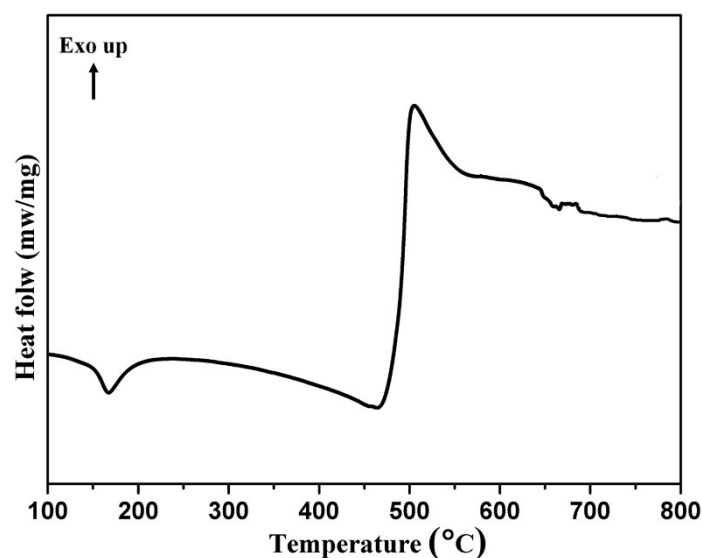


Fig. S10. DSC curve of pure PVDF film.

12. TGA-DSC test of Al₂O₃/PVDF films

The average diameter of Al₂O₃ used is 50 nm. The preparation process of Al₂O₃/PVDF films is the same as that of Al/PVDF films and the content of Al₂O₃ is 50% to ensure there are enough Al₂O₃ to react with PVDF. The TGA-DSC test is conducted from 50 to 700 °C with a heating rate of 20 °C min⁻¹ under a nitrogen flow

rate of 50 mL min^{-1} and the result is shown in **Fig. S11**.

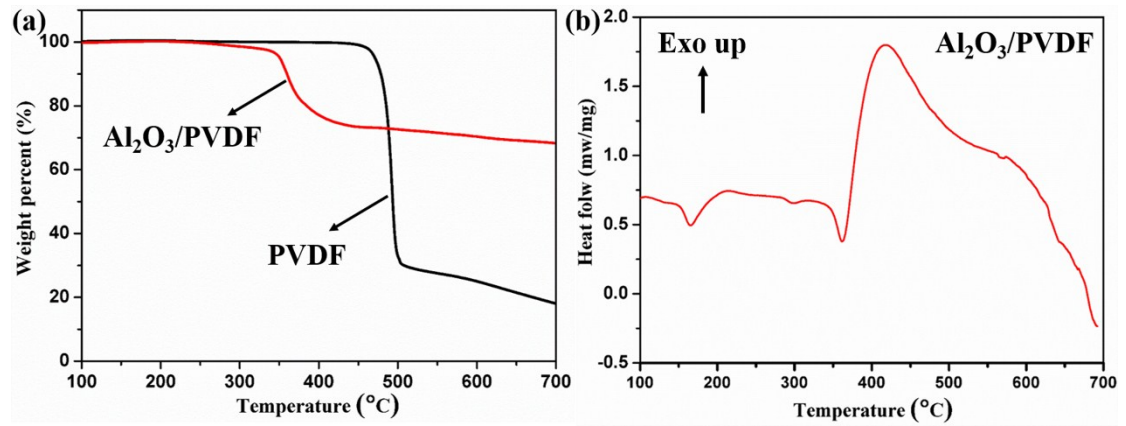


Fig. S11. (a) TGA curves of PVDF and $\text{Al}_2\text{O}_3/\text{PVDF}$ films, (b) DSC curve of $\text{Al}_2\text{O}_3/\text{PVDF}$ films.

13. Optical signal during the combustion process

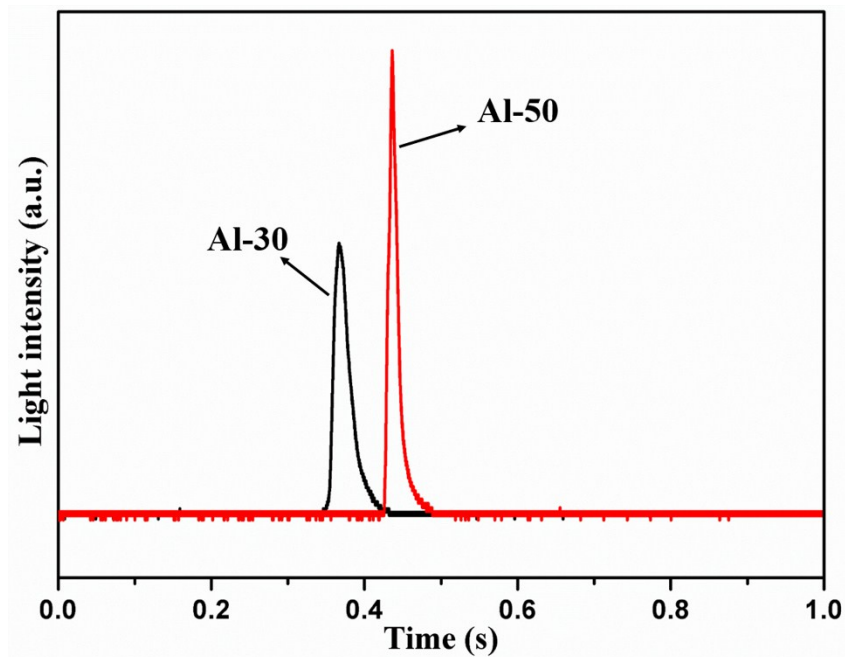


Fig. S12. Time-solved light intensity of different samples.